Handout 3: decaying MHD turbulence

An important problem in primordial magnetogenesis are the small length scales. This is where the possibility of an inverse cascade plays a role. To get into that, we first need to define spectra. This will be done next.

1 Energy spectra

We define magnetic energy and magnetic helicity spectra, $E_{\rm M}(k,t)$ and $H_{\rm M}(k,t)$, as shell-integrals.

$$E_{\rm M}(k) = \tfrac{1}{2}\sum_{k_-<|\boldsymbol{k}|\le k_+}|\tilde{\boldsymbol{B}}(\boldsymbol{k})|^2, \tag{1}$$

$$H_{\rm M}(k) = \tfrac{1}{2}\sum_{k_-<|\boldsymbol{k}|\le k_+}(\tilde{\boldsymbol{A}}\cdot\tilde{\boldsymbol{B}}^*+\tilde{\boldsymbol{A}}^*\cdot\tilde{\boldsymbol{B}}), \tag{2}$$

where $k_\pm=k\pm\delta k/2$ and $\delta k=2\pi/L$ is the wavenumber increment and also the smallest wavenumber in the plane L^2 with L being the size of the magnetograms.

Note that the magnetic helicity spectrum is not the spectrum of $\boldsymbol{A}\cdot\boldsymbol{B}$, although that one also plays a certain role. That one would be called the magnetic helicity variance spectrum. It will be needed in connection with the Hosking integral, an important quantity discussed below.

Sometimes, we call magnetic energy spectra $M(k)$ and magnetic helicity spectra $H(k)$. We also have *kinetic*energy and helicity spectra.

2 Realizability condition

It is convenient to decompose the Fourier transformed magnetic vector potential, $\boldsymbol{A}_{\boldsymbol{k}}$, into a longitudinal component, $\boldsymbol{h}^{\parallel}$, and eigenfunctions $\boldsymbol{h}^{\pm}$ of the curl operator. Especially in the context of spherical domains these eigenfunctions are also called Chandrasekhar–Kendall functions, while in Cartesian domains they are usually referred to as Beltrami waves. This decomposition has been used in studies of turbulence and in magnetohydrodynamics and in dynamo theory. Using this decomposition we can write the Fourier transformed magnetic vector potential as

$$\boldsymbol{A}_{\boldsymbol{k}}=a^+_{\boldsymbol{k}}\boldsymbol{h}^+_{\boldsymbol{k}}+a^-_{\boldsymbol{k}}\boldsymbol{h}^-_{\boldsymbol{k}}+a^{\parallel}_{\boldsymbol{k}}\boldsymbol{h}^{\parallel}_{\boldsymbol{k}}, \tag{3}$$

with

$$\mathrm{i}\boldsymbol{k}\times\boldsymbol{h}^{\pm}_{\boldsymbol{k}}=\pm k\boldsymbol{h}^{\pm}_{\boldsymbol{k}},\qquad k=|\boldsymbol{k}|, \tag{4}$$

and

$$\langle\boldsymbol{h}^{+*}_{\boldsymbol{k}}\cdot\boldsymbol{h}^{+}_{\boldsymbol{k}}\rangle=\langle\boldsymbol{h}^{-*}_{\boldsymbol{k}}\cdot\boldsymbol{h}^{-}_{\boldsymbol{k}}\rangle=\langle\boldsymbol{h}^{\parallel *}_{\boldsymbol{k}}\cdot\boldsymbol{h}^{\parallel}_{\boldsymbol{k}}\rangle=1, \tag{5}$$

where asterisks denote the complex conjugate, and angular brackets denote, as usual, volume averages. The longitudinal part $a^{\parallel}_{\boldsymbol{k}}\boldsymbol{h}^{\parallel}_{\boldsymbol{k}}$ is parallel to $\boldsymbol{k}$ and vanishes after taking the curl to calculate the magnetic field. In the Coulomb gauge, $\nabla\cdot\boldsymbol{A}=0$, the longitudinal component vanishes altogether.

The (complex) coefficients $a^{\pm}_{\boldsymbol{k}}(t)$ depend on $\boldsymbol{k}$ and t, while the eigenfunctions $\boldsymbol{h}^{\pm}_{\boldsymbol{k}}$, which form an orthonormal set, depend only on $\boldsymbol{k}$ and are given by

$$\boldsymbol{h}^{\pm}_{\boldsymbol{k}}=\frac{1}{\sqrt{2}}\frac{\boldsymbol{k}\times(\boldsymbol{k}\times\boldsymbol{e})\mp\mathrm{i}k(\boldsymbol{k}\times\boldsymbol{e})}{k^2\sqrt{1-(\boldsymbol{k}\cdot\boldsymbol{e})^2/k^2}}, \tag{6}$$

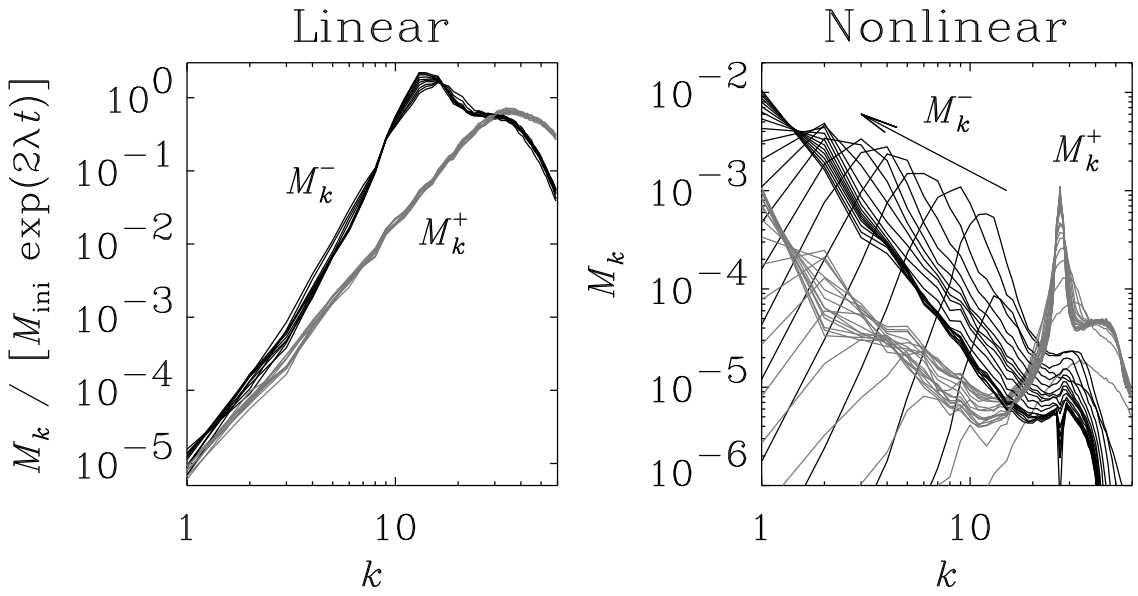

Figure 1: Power spectra of magnetic energy of positively and negatively polarized parts (M_k^+ and M_k^-) in the linear and nonlinear regimes. The spectra in the linear regime have been compensated by the exponential growth factor to make them collapse on top of each other. Here the forcing wavenumber is in the dissipative subrange, $k_{\rm f} = 27$, but this allows enough scale separation to see the inverse transfer of magnetic energy to smaller k.

where $\boldsymbol{e}$ is an arbitrary unit vector that is not parallel to $\boldsymbol{k}$. With these preparations we can write the magnetic helicity and energy spectra in the form

$$H_k = k(|a_k^+|^2 - |a_k^-|^2)V, \tag{7}$$

$$M_k = \tfrac{1}{2}k^2(|a_k^+|^2 + |a_k^-|^2)V, \tag{8}$$

where V is the volume of integration. (Here again the factor μ_0^{-1} is ignored in the definition of the magnetic energy.) From Equations (7) and (8) one sees that

$$\tfrac{1}{2}k|H_k| \le M_k, \tag{9}$$

which is also known as the *realizability condition*. A fully helical field has therefore $M_k = \pm\frac{1}{2}kH_k$.

For further reference we now define power spectra of those components of the field that are either right or left handed, i.e.

$$H_k^\pm = \pm k|a_k^\pm|^2 V, \quad M_k^\pm = \tfrac{1}{2}k^2|a_k^\pm|^2 V. \tag{10}$$

Thus, we have $H_k = H_k^+ + H_k^-$ and $M_k = M_k^+ + M_k^-$. Note that $H_k^\pm$ and $M_k^\pm$ can be calculated without explicit decomposition into right and left handed field components using

$$H_k^\pm = \tfrac{1}{2}(H_k \pm 2k^{-1}M_k), \quad M_k^\pm = \tfrac{1}{2}(M_k \pm \tfrac{1}{2}kH_k). \tag{11}$$

This method is significantly simpler than invoking explicitly the decomposition in terms of $a_{\boldsymbol{k}}^\pm \boldsymbol{h}_{\boldsymbol{k}}^\pm$.

In Figure **??**, we show plots of $M_k^\pm$ in connection with turbulence simulations. Here the turbulence is driven with a helical forcing function proportional to $\boldsymbol{h}_{\boldsymbol{k}}^+$; see Equation (6).

The integral realizability condition can be obtained by integrating, but first we write

$$-2k^{-1}M_k < H_k < 2k^{-1}M_k, \tag{12}$$

and then we define the integral scale

$$\xi_{\rm M} = \int k^{-1}M_k \,{\rm d}k \Big/ \int M_k \,{\rm d}k. \tag{13}$$

3 Frisch argument

The occurrence of an inverse cascade can be understood as the result of two waves (wavenumbers $\boldsymbol{p}$ and $\boldsymbol{q}$) interacting with each other to produce a wave of wavenumber $\boldsymbol{k}$. The following argument is due to Frisch et al. (1975). Assuming that during this process magnetic energy is conserved together with magnetic helicity, we have

$$M_p + M_q = M_k, \tag{14}$$

$$|H_p| + |H_q| = |H_k|, \tag{15}$$

where we are assuming that only helicity of one sign is involved. Suppose the initial field is fully helical and has the same sign of magnetic helicity at all scales, we have

$$2M_p = p|H_p| \quad \text{and} \quad 2M_q = q|H_q|, \tag{16}$$

and so Equation (14) yields

$$p|H_p| + q|H_q| = 2M_k \geq k|H_k|, \tag{17}$$

where the last inequality is just the realizability condition (9) applied to the target wavenumber $\boldsymbol{k}$ after the interaction. Using Equation (15) in Equation (17) we have

$$p|H_p| + q|H_q| \geq k(|H_p| + |H_q|). \tag{18}$$

In other words, the target wavevector $\boldsymbol{k}$ after the interaction of wavenumbers $\boldsymbol{p}$ and $\boldsymbol{q}$ satisfies

$$k \leq \frac{p|H_p| + q|H_q|}{|H_p| + |H_q|}. \tag{19}$$

The expression on the right hand side of Equation (19) is a weighted mean of p and q and thus satisfies

$$\min(p,q) \leq \frac{p|H_p| + q|H_q|}{|H_p| + |H_q|} \leq \max(p,q), \tag{20}$$

and therefore

$$k \leq \max(p,q). \tag{21}$$

In the special case where $p = q$, we have $k \leq p = q$, so the target wavenumber after interaction is always less or equal to the initial wavenumbers. In other words, wave interactions tend to transfer magnetic energy to smaller wavenumbers, i.e. to larger scale. This corresponds to an inverse cascade. The realizability condition, $\frac{1}{2}k|H_k| \leq M_k$, was the most important ingredient in this argument. An important assumption that we made in the beginning was that the initial field be fully helical.

4 Initial spectrum

A random field with white noise is delta-correlated in real space and a constant in $\boldsymbol{k}$-space. Remember that the magnetic energy spectrum is shell-integrated. Therefore, in 3-D, the volume of the shell is $4\pi k^2 \delta k$, so the spectrum increases like k^2. (In 2-D, spectra of white noise only increase proportional to k, and they would be flat in 1-D.)

A random magnetic field must also obey $\boldsymbol{\nabla} \cdot \boldsymbol{B} = 0$. Therefore, $\boldsymbol{A}$ must be random and it would have a k^2 spectrum. Since the spectrum is quadratic in the field, the spectrum of $\boldsymbol{B}$ is then proportional to k^4. Such spectra are also called *causal spectra* (Durrer & Caprini, 2003).

5 Decaying turbulence laws from dimensional arguments

A famous dimensional argument is that to obtain the scaling of the Kolmogorov spectrum. There one says that the physics of the Kolmogorov cascade is characterized by the energy flux, ϵ_K, which has dimensions of $\mathrm{cm}^2\,\mathrm{s}^{-3}$. The kinetic energy spectrum $E_{\rm K}(k)$ itself has dimensions $\mathrm{cm}^3\,\mathrm{s}^{-2}$. One assumes that it is a power law of k, and that ϵ_K enters also, so then we have

$$E_{\rm K}(k) = \mathrm{const} \times \epsilon_K^a k^b, \tag{22}$$

so you have two equations for the dimensions cm and s, respectively, for two unknowns, a and b.

By a similar argument, you can also an equation for a length length scale:

$$\xi_{\rm M}(t) \propto I_{\rm M}^{1/3}\, t^{2/3}, \tag{23}$$

where defined $I_{\rm M} = \langle \boldsymbol{A} \cdot \boldsymbol{B} \rangle$, and similarly for $E_{\rm M}(k)$, i.e.,

$$\mathcal{E}_{\rm M}(t) \propto I_{\rm M}^{2/3}\, t^{-2/3}. \tag{24}$$

Finally, one can also find an expression for the envelope of the spectrum:

$$E_{\rm M}(k,t) \lesssim \mathrm{const} \times\ I_{\rm M}. \tag{25}$$

For nonhelical turbulence, however, we believe that the relevant conserved quantity is the Hosking integral, which will be introduced next.

6 Anastrophy in 2-D

In strict 2-D, as opposed to what is sometimes called 2.5-D (which is also just 2-D, but now the magnetic field also has a component out of the place), the anastrophy is $\langle A_z^2 \rangle$ is conserved. Here, $A_z(x,y,t)$ is the z component of the magnetic vector potential (and the other two vanish). The 2-D case can more easily be run and is therefore suitable for exercises:

- What scaling do you expect in strict 2-D where the decay is controlled by the conservation of $\langle A_z^2 \rangle$?
- Run the codes for different box sizes L. (In the code, we give $k_1 = 2\pi/L$, which is called wav1 and is unity by default.)
- Vary the amplitude. Check that all the runs fall on a line close to $v_{\rm A} = \xi_{\rm M}/t$ at the time t.

7 Hosking integral

The Hosking integral $I_{\rm H}$ is defined as the asymptotic limit of the magnetic helicity density correlation integral,

$$\mathcal{I}_{\rm H}(R) = \int_{V_R} \langle h(\boldsymbol{x}) h(\boldsymbol{x}+\boldsymbol{r}) \rangle\, \mathrm{d}^3 r, \tag{26}$$

for scales R large compared with the correlation length $\xi_{\rm M}$ of the turbulence, but small compared with the system size L. Here, $V_R = 4\pi R^3/3$ is the volume of a sphere of radius R. For small values of R, the function $\mathcal{I}_{\rm H}(R)$ increases proportional to R^3, but for large R, it levels off when there is no net magnetic helicity. However, as explained in **?**, this is different for finite magnetic helicity, as is discussed below. In practice, the value of R is chosen empirically and must always be small compared with the size of the domain.

? devised and compared different methods for computing $\mathcal{I}_{\rm H}(R)$. These methods are all based on the Fourier transform of h. Particularly simple is what they called the box-counting method for a spherical volume with radius R. This allowed them to rewrite Equation (26) as a weighted integral over $\mathrm{Sp}(h)$,

$$\mathcal{I}_{\rm H}(R) = \int_0^\infty w(k,R)\,\mathrm{Sp}(h)\,\mathrm{d}k, \tag{27}$$

where

$$w(k,R) = \frac{4\pi R^3}{3}\left[\frac{6j_1(kR)}{kR}\right]^2, \tag{28}$$

and $j_1(x) = (\sin x - x\cos x)/x^2$ is a spherical Bessel function.

8 Enpoints

Magnetically dominated turbulence is characterized by the turbulent magnetic energy density $\mathcal{E}_{\rm M}$ and the magnetic integral scale $\xi_{\rm M}$. Both $\mathcal{E}_{\rm M}(t)$ and $\xi_{\rm M}(t)$ can be defined in terms of the magnetic energy spectrum $E_{\rm M}(k,t)$, such that $\mathcal{E}_{\rm M} = \int E_{\rm M}\,\mathrm{d}k$ and $\xi_{\rm M} = \int k^{-1}E_{\rm M}\,\mathrm{d}k/\mathcal{E}_{\rm M}$. In decaying turbulence, both quantities depend algebraically rather than exponentially on time. Therefore, the decay is primarily characterized by power laws,

$$\mathcal{E}_{\rm M} \propto t^{-p} \quad \text{and} \quad \xi_{\rm M} \propto t^q, \tag{29}$$

rather than by exponential laws of the type $\mathcal{E}_{\rm M} \propto e^{-t/\tau}$. The algebraic decay is mainly a consequence of nonlinearity. On the other hand, in decaying hydromagnetic turbulence with significant cross-helicity, for example, the nonlinearity in the induction equation is reduced and then the decay is indeed no longer algebraic, but closer to exponential.

An obvious difference between algebraic and exponential decays is that in the former $\mathcal{E}_{\rm M}(t)$ is characterized by the nondimensional quantity p, while in the latter it is characterized by the dimensionful quantity τ. Following Hosking & Schekochihin (2023), a decay time τ can also be defined for an algebraic decay and is then given by

$$\tau^{-1} = -\mathrm{d}\ln\mathcal{E}_{\rm M}/\mathrm{d}t. \tag{30}$$

In the present case of a power-law decay, this value of $\tau = \tau(t)$ is time-dependent and can be related to the instantaneous decay exponent

$$p(t) = -\mathrm{d}\ln\mathcal{E}_{\rm M}/\mathrm{d}\ln t \tag{31}$$

through $\tau = t/p(t)$ (i.e., no new parameter emerges except for t itself). However, a useful way of incorporating new information is by relating τ to the Alfvén time $\tau_{\rm A} = \xi_{\rm M}/v_{\rm A}$ through

$$\tau = C_{\rm M}\xi_{\rm M}/v_{\rm A}, \tag{32}$$

where $C_{\rm M}$ is a nondimensional parameter, and $v_{\rm A}$ is the Alfvén velocity, which is related to the magnetic energy density through $\mathcal{E}_{\rm M} = B_{\rm rms}^2/2\mu_0 = \rho v_{\rm A}^2/2$, where ρ is the density, μ_0 the vacuum permeability, and $B_{\rm rms}$ the root mean square (rms) magnetic field.

As was noted by Hosking & Schekochihin (2023), Equation (32) can be used to define the endpoints of the evolutionary tracks in a diagram of $B_{\rm rms}$ versus $\xi_{\rm M}$ or, equivalently, $v_{\rm A}$ versus $\xi_{\rm M}$ (i.e., $v_{\rm A} = v_{\rm A}(\xi)$). They also noted that the location of these endpoints is sensitive to whether or not $C_{\rm M}$ depends on the resistivity of the plasma. If it does depend on the resistivity, this could be ascribed to the effects of magnetic reconnection, which might slow down the turbulent decay.

Magnetic reconnection refers to a change in magnetic field line connectivity that is subject to topological constraints. A standard example is x-point reconnection, which becomes slower as the x-point gets degenerated into an extremely elongated structure (Parker, 1957). It is usually believed that in the presence of turbulence, such structures break up into progressively smaller ones, which makes reconnection eventually fast (i.e., independent of the microphysical resistivity). However, whether this would

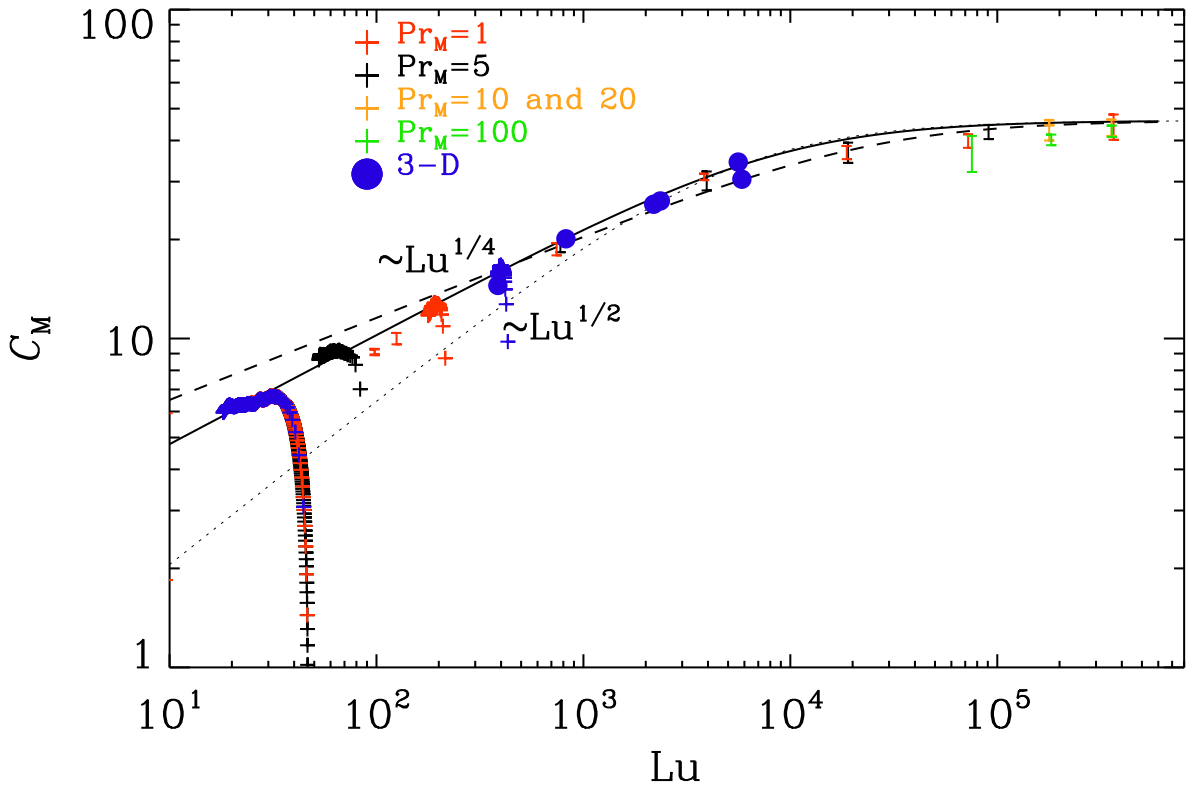

Figure 2: Dependence of $C_{\rm M}$ on Lu for the 2D runs. Shallow scaling $\propto {\rm Lu}^{0.1}$ is found for $10^4 < {\rm Lu} < 10^5$. The black (red) data points are for ${\rm Pr}_M = 5$ (${\rm Pr}_M = 1$). The blue data points denote 3D results. The orange symbols are for the runs with ${\rm Pr}_M = 10$ and 20. The dashed and dotted lines give show ${\rm Lu}^{1/2}$ and ${\rm Lu}^{1/4}$ scalings for small values of Lu. Adapted from Brandenburg et al. (2024), but now together with the new data for small values of Lu, which indicated a clear 1/3 scaling (solid line).

also imply that τ becomes independent of the resistivity remains an unclear issue. Another question concerns the speed at which magnetic flux can be processed through a current sheet. Also of interest is the timescale on which the topology of the magnetic field changes. These different timescales may not all address the value of $C_{\rm M}$ that relates the decay time to the Alfvén time.

In magnetically dominated turbulence, the effect of the resistivity is quantified by the Lundquist number. For decaying turbulence, it is time-dependent and defined as

$$ {\rm Lu}(t) = v_{\rm A}(t)\,\xi_{\rm M}(t)/\eta. \tag{33}$$

This quantity is similar to the magnetic Reynolds number if we replace $v_{\rm A}$ by the rms velocity, $u_{\rm rms}$. Here, however, the plasma is driven by the Lorentz force, so the Lundquist number is a more direct way of quantifying the resistivity than the magnetic Reynolds number. The Alfvénic Mach number is defined as ${\rm Ma}_{\rm A} = u_{\rm rms}/v_{\rm A}$.

Although 2D and 3D runs are in many ways rather different from each other, we now determine the same diagnostics as in the 3D case (see Figure 2 for a plot of $C_{\rm M}$ versus Lu). We see that the $C_{\rm M}$ dependence on Lu is qualitatively similar for 2D and 3D turbulence.

We note that our definition of $\xi_{\rm M}$ does not include a 2π factor. A comparison with the Sweet–Parker value of $n = 1/2$ results in reasonable agreement for small values of Lu, but there are rather noticeable departures from the data for intermediate values.

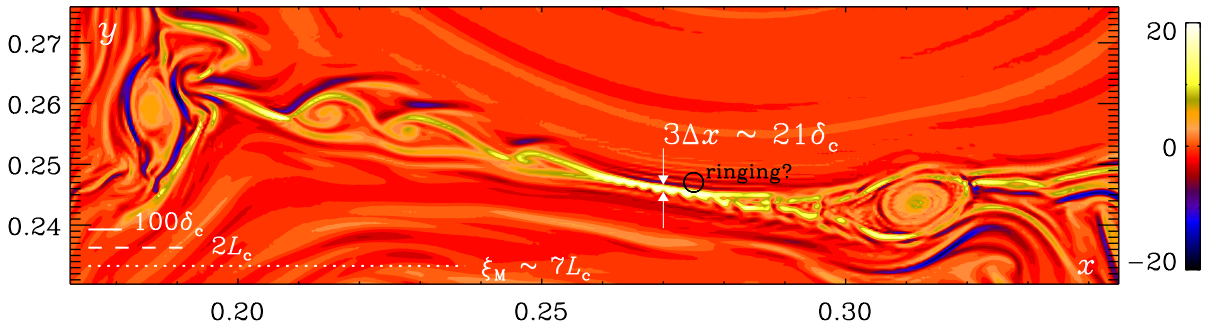

Figure 3: Visualization of $J_z(x,y)$ of Run 2m6 with $\mathrm{Pr}_M = 10$, $\mathrm{Lu} = 1.8\times10^5$, $\mathrm{Lu}_\nu \approx 5\times10^4$, and 16384^2 mesh points at $t = 464$ for a small part of the domain with sizes $2.8\xi_\mathrm{M}(t)\times0.74\xi_\mathrm{M}(t)$. The lengths of $100\,\delta_\mathrm{c}$, $2L_\mathrm{c}$, and ξ_M are indicated by horizontal white solid, dashed, and dotted lines, respectively. The thickness of the current sheet corresponds to about $3\Delta x \approx 21\,\delta_\mathrm{c}$. In its proximity, there are also indications of ringing, indicated by the black circle.

Figure 3 a visualization of $J_z(x,y)$ for Run 2m6 with $\mathrm{Pr}_M = 10$ and 16384^2 mesh points at $t = 464$ for a small part of the domain with sizes $2.8\xi_\mathrm{M}(t)\times0.74\xi_\mathrm{M}(t)$ where a large current sheet breaks up into smaller plasmoids. A comparison between Runs 2m5 and 2m6 with 8192^2 and 16384^2 in Brandenburg et al. (2024).

References

Brandenburg, A., Neronov, A., & Vazza, F., "Resistively controlled primordial magnetic turbulence decay," *Astron. Astrophys.* **687**, A186 (2024).

Durrer, R., & Caprini, C., "010," *J. Cosm. Astrop. Phys.* **JCAP**, 0311 (2003). Primordial magnetic fields and causality

Frisch, U., Pouquet, A., Léorat, J., & Mazure, A., "Possibility of an inverse cascade of magnetic helicity in hydrodynamic turbulence," *J. Fluid Mech.* **68**, 769–778 (1975).

Hosking, D. N., & Schekochihin, A. A., "Cosmic-void observations reconciled with primordial magnetogenesis," *Nat. Comm.* **14**, 7523 (2023).

Kahniashvili, T., Tevzadze, A. G., Brandenburg, A., & Neronov, A., "Evolution of primordial magnetic fields from phase transitions," *Phys. Rev. D* **87**, 083007 (2013).

Parker, E. N., "Sweet's Mechanism for Merging Magnetic Fields in Conducting Fluids," *J. Geophys. Res.* **62**, 509–520 (1957).

$Header: /var/cvs/brandenb/tex/teach/COSMOMAG26/3_decaying_turbulence/notes.tex,v 1.10 2026/01/14 13:11:44 brandenb Exp $